

Contents lists available at ScienceDirect

# Petroleum Science

journal homepage: www.keaipublishing.com/en/journals/petroleum-science



# **Original Paper**

# Research on the in-situ catalytic pyrolysis of heavy oil by 2D layered MOF and its catalytic mechanism



Chi Li  $^{a,\,b}$ , Ji-Xiang Guo  $^{a,\,b,\,*}$ , Li Wang  $^{a,\,b}$ , Wen-Long Zhang  $^{a,\,b}$ , Peng-Cheng Xue  $^{a,\,b}$ , Chen-Hao Gao  $^{a,\,b}$ 

- <sup>a</sup> State Key Laboratory of Heavy Oil Processing, China University of Petroleum (Beijing), Beijing, 102249, China
- <sup>b</sup> Unconventional Petroleum Research Institute, China University of Petroleum (Beijing), Beijing, 102249, China

#### ARTICLE INFO

#### Article history Received 27 November 2024 Received in revised form 12 March 2025 Accepted 23 April 2025 Available online 29 April 2025

Edited by Min Li

Keywords: 2D MOF In-situ catalytic technology Heavy oil Catalytic upgrading Molecular dynamics

#### ABSTRACT

China possesses abundant heavy oil resources, yet faces challenges such as high viscosity, underdeveloped production technologies, and elevated development cost. Although the in-situ catalytic viscosityreduction technology can address certain technical, environmental, and cost problems during the extraction process, the catalysts often suffer from poor stability and low catalytic efficiency. In this study, a green and simple room-temperature stirring method was employed to synthesize a class of highly efficient and stable 2D MOF catalysts, which possess the capability to conduct in-situ catalytic pyrolysis of heavy oil and reduce the viscosity. Under the condition of 160 °C, a catalyst concentration of 0.5 wt%, and a hydrogen donor (tetralin) concentration of 2 wt%, the viscosity-reduction rate of Fe-MOF is as high as 89.09%, and it can decrease the asphaltene content by 8.42%. In addition, through the structural identification and analysis of crude oil asphaltenes, the causes for the high viscosity of heavy oil are explained at the molecular level. Through the analysis of catalytic products and molecular dynamics simulation, the catalytic mechanism is studied. It is discovered that Fe-MOF can interact with heavy oil macromolecules via coordination and pore-channel effects, facilitating their cracking and dispersal. Furthermore, synergistic interactions between Fe-MOF and the hydrogen donor facilitates hydrogenation reactions and enhances the viscosity-reducing effect. This study provides a novel strategy for boosting heavy oil recovery and underscores the potential of 2D MOFs in catalytic pyrolysis applications. © 2025 The Authors. Publishing services by Elsevier B.V. on behalf of KeAi Communications Co. Ltd. This is an open access article under the CC BY-NC-ND license (http://creativecommons.org/licenses/by-nc-nd/

4.0/).

## 1. Introduction

With the growing global energy demand, petroleum remains a primary energy source, playing a vital role in the global economy and energy security due to its supply dynamics and advancements in extraction technologies. As conventional petroleum resources become increasingly depleted, research and industrial efforts have shifted toward unconventional resources, particularly heavy and extra-heavy oil, which have emerged as key targets for global petroleum development (Guo et al., 2024; Khorasani et al., 2022; Xue et al., 2022). However, the inherently low mobility of heavy oil poses substantial technical barriers to its extraction and transportation. Advanced in-situ catalytic pyrolysis has gained prominence as a viable alternative to conventional extraction

technologies, overcoming their inherent limitations. By introducing specific catalysts into oil reservoirs, this technology initiates chemical reactions that significantly reduce the apparent viscosity of heavy oil and enhance its recovery rate. It offers a promising strategy for the efficient development and utilization of heavy oil resources, which can maximize energy conservation and environmental sustainability (Elahi et al., 2019; Scheele-Ferreira et al., 2017).

Conventional catalysts widely used in heavy oil pyrolysis include transition metal salts (Zhou et al., 2024), supported catalysts (Li et al., 2021), zeolites (Goshayeshi et al., 2024), and metal oxides (Mukhamatdinov et al., 2023). Despite their widespread use, these catalysts are often limited by issues such as poor stability, susceptibility to deactivation, and the requirement for stringent reaction conditions. These challenges highlight the urgent need for developing catalysts that exhibit high activity, enhanced stability, and reliable performance under practical operating conditions (Karnjanakom et al., 2017; Lin et al., 2019; Zhang et al., 2022). Li et al. (2024) proposed that nanocatalysts, due to their ability to

E-mail address: guojx003@126.com (J.-X. Guo).

Peer review under the responsibility of China University of Petroleum (Beijing).

<sup>\*</sup> Corresponding author.

migrate through oil reservoir microchannels and disperse efficiently in heavy oil, exhibit superior catalytic efficiency for in-situ upgrading. Liang et al. (2023) suggested that merely modulating the metal active centers of catalysts is insufficient to meet practical requirements. Instead, nanoscale multifunctional ordered assembly and coordination offer a more effective approach. Compared to conventional catalysts for heavy oil pyrolysis, 2D metal-organic frameworks (MOFs) exhibit higher specific surface areas, tailorable pore architectures, and multifunctional active sites (Lin et al., 2021; Wang et al., 2023; Wang and Astruc, 2020; Xue et al., 2021). Currently, research into MOF catalysts for heavy oil viscosity reduction remains relatively limited. L. Wang et al. (2024) synthesized Co-MOF and Ni-MOF catalysts and performed viscosity reduction experiments with crude oil from Shengli Oilfield. The results demonstrated that the Ni-MOF catalyst achieved a viscosity reduction rate of 91.97% after reacting at 280 °C for 24 h, along with significant reductions in asphaltene and resin contents. In another study, Razavian and Fatemi (2021) applied Mo-doped MAF-6 MOF to reduce the viscosity of crude oil from Tehran Petroleum Refinery Corporation, achieving a 37% viscosity reduction after reaction at 350 °C for 210 min. These studies indicate that MOF catalysts show significant potential for the in-situ catalytic pyrolysis of heavy oil. Future research should focus on improving catalyst stability and reducing the required reaction temperature to enhance practical applications.

To promote the design and development of heavy oil pyrolysis catalysts, researchers have been exploring the mechanisms of viscosity reduction catalyzed by heavy oil (Li et al., 2024). Using molecular dynamics simulations, C.H. Wang et al. (2024) thoroughly investigated the viscosity reduction mechanism of surfacefunctionalized Fe<sub>3</sub>O<sub>4</sub> nanoparticles in heavy oil. Their findings revealed that this catalyst primarily disrupts the aggregation structures of asphaltenes, thereby influencing their aggregate size and diffusion properties. Additionally, it reduces the interaction energy between asphaltenes, as well as the number and strength of hydrogen bonds. Zhou et al. (2025) conducted a comprehensive review of the viscosity reduction mechanisms of heavy oil, categorized three dominant pathways: the carbocation reaction mechanism, dominant at lower temperatures; the free-radical reaction mechanism, dominant at higher temperatures; and the coexistence of both mechanisms. with the type of mechanism largely determined by the catalyst. Owing to the compositional complexity of heavy oil components, elucidating the viscosity reduction mechanisms remains challenging. Future research should focus on further analyzing multi-component complex structures. Furthermore, the mechanism of action of hydrogen donors remains controversial and requires further investigation.

In this study, 2D Fe-MOF and Cu-MOF were synthesized, and their catalytic performance in heavy oil pyrolysis and resultant viscosity reduction effects were systematically evaluated. Through kinetic analysis, the mechanism by which MOF catalysts influence heavy oil pyrolysis was thoroughly investigated. Based on the results of catalytic pyrolysis experiments, the potential action mechanisms of these catalysts were proposed. This study offers innovative technical approaches and practical pathways for the efficient and environmentally sustainable extraction of heavy oil.

# 2. Experiments and methodology

# 2.1. Materials and reagents

All reagents employed in the investigation were of analytical quality. Including Cupric nitrate hexahydrate ( $Cu(NO_3)_2 \cdot 6H_2O$ ), ferric nitrate nonahydrate ( $Fe(NO_3)_3 \cdot 9H_2O$ ), N,N-Dimethylformamide (DMF), terephthalic acid ( $H_2BDC$ ), trimesic

acid ( $H_3BTC$ ), triethanolamine (TEA), acetone ( $C_3H_6O$ ) and anhydrous ethanol ( $C_2H_5OH$ ) purchased from Aladdin Chemical Reagent Company. In addition, deionized water was used in the experiment.

Heavy oil samples were taken from Tahe Oilfield, China. The basic properties of heavy oil are shown in Table 1.

#### 2.2. Characterization

The morphology and structure of the MOF catalyst were investigated by using scanning electron microscopy (SEM) and transmission electron microscopy (TEM). The functional groups and structures of the MOF catalyst and heavy oil asphaltene were characterized by using Fourier transform infrared spectroscopy (FTIR) and X-ray diffraction (XRD). The bonding mode and elemental valence state of the MOF catalyst were characterized by using X-ray photoelectron spectroscopy (XPS). The thermal stability of the MOF catalyst was assessed by using thermogravimetric analysis (TG).

## 2.3. Identification of the structure of asphaltene in crude oil

The composition of different types of heteroatomic compounds in heavy oil was analyzed by employing Fourier transform ion cyclotron resonance mass spectrometry (FT-ICR MS) and Electrospray ionization (ESI) technique. Under the +ESI mode, nitrogencontaining compounds (such as amines, alkaloids, etc.) and hydroxyl-containing compounds (such as alcohols, phenols, etc.) in crude oil are mainly detected. Under the -ESI mode, acidic compounds containing carboxyl groups, sulfonic acid groups, etc. in crude oil are mainly detected. Based on the double-bond equivalent (DBE) and relative abundance, the asphaltene structures of different heteroatom types in heavy oil are mainly deduced (Zhang et al., 2023).

## 2.4. Preparation and synthesis of catalyst

In this study, a 2D MOF catalyst was synthesized through a simple and green method of stirring at room temperature (Ge et al., 2021). The preparation process is illustrated in Fig. 1. Firstly, 0.48 g of  $\text{Cu}(\text{NO}_3)_2 \cdot 3\text{H}_2\text{O}$  and 0.24 g of  $\text{H}_3\text{BTC}$  were dissolved in 60 mL of a mixed solvent composed of deionized water, ethanol, and DMF in a volume ratio of 1:1:1, and then received ultrasonic treatment for 30 min to ensure full dissolution and mixing. Subsequently, 10 mL of TEA was added, and the mixture was stirred at room temperature for 24 h. After centrifugal sedimentation, it was continuously stirred in acetone for 5 h. After the product was collected by centrifugation, it was washed several times with ethanol and dried to obtain the 2D Cu-MOF. Meanwhile, Fe-MOF was synthesized by a similar approach.

## 2.5. Catalytic experiment of heavy oil

Heavy oil and water were mixed in a ratio of 7:3 and then added into a high-temperature and high-pressure reactor equipped with a stirring device to simulate the actual reservoir conditions.

**Table 1** Basic properties of heavy oil.

Property	Value	Property	Value
Density, g⋅cm <sup>-3</sup>	1.05	Fe, ppm	28
Saturated, %	19.87	Ni, ppm	35
Aromatic, %	21.77	V, ppm	218
Resin, %	13.28	Na, ppm	67
Asphaltene, %	45.08	Ca, ppm	20

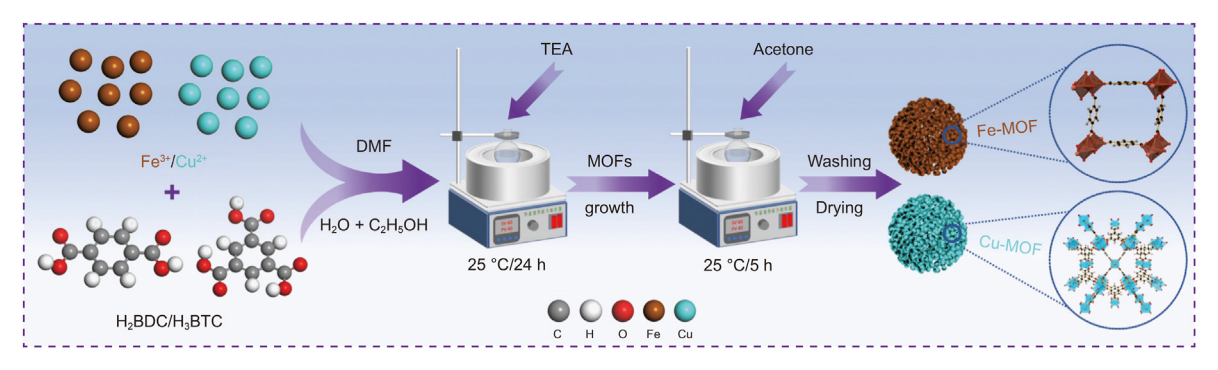


Fig. 1. Synthetic schematic diagram of MOF catalyst.

Subsequently, 0.5% by mass of MOF catalyst and 2% by mass of tetralin were added to it. Before the start of the reaction, nitrogen was introduced into the high-temperature and high-pressure reactor at a flow rate of 100 mL/min for 15 min for purging and evacuation treatment to prevent oxygen from influencing the experimental results. Meanwhile, nitrogen was continuously introduced throughout the reaction process to maintain the required pressure. The temperature was raised to 160 °C, and the reaction was conducted for 24 h. After the reaction was completed, it was naturally cooled to room temperature to obtain the catalytically pyrolyzed heavy oil. Subsequently, the resulting mixture was subjected to dehydration treatment after sedimentation and centrifugation.

Then, the viscosity of the heavy oil before and after the reaction was measured and compared by using a HAAKE MARS III rheometer (HAAKE, Germany). The shear rate was 7.2 s<sup>-1</sup>. The viscosity reduction rate (VRR) after the catalytic reaction was calculated based on the viscosity results as follows Eq. (1):

$$VRR(\%) = \frac{\eta_0 - \eta_1}{\eta_0} \times 100\% \tag{1}$$

In this context,  $\eta_0$  (mPa·s) is the initial viscosity of the heavy oil; and  $\eta_1$  (mPa·s) is the viscosity of the heavy oil after catalytic viscosity reduction.

In addition, the composition of saturates, aromatics, resins and asphaltenes (SARA) of heavy oil before and after the catalytic reaction was determined respectively by employing the method based on thin-layer chromatography, and the changes in the contents of the four components before and after catalytic pyrolysis were quantitatively analyzed. Meanwhile, elemental analysis, Gas Chromatography-Mass Spectrometry (GC-MS) and other analyses were also performed on the crude oil before and after catalysis.

## 2.6. Pyrolysis kinetics

A study from a kinetic perspective can lead to a better understanding of the reaction process and an evaluation of the catalyst's performance. For this purpose, the relevant kinetic parameter calculations for the pyrolysis process were carried out. Common models used to describe the viscosity-temperature relationship of crude oil encompass the Arrhenius-type model, the Williams-Landel-Ferry (WLF) equation, etc. In this study, the Arrhenius equation Eq. (2) was employed to fit the viscosity-temperature data, and the fitted equation is presented as Eq. (3):

$$k = A \cdot e^{\frac{-E}{RT}} \tag{2}$$

$$\eta = B \cdot e^{\frac{\Delta E}{RT}} \tag{3}$$

In the equation, k is the reaction rate constant; A is the preexponential factor;  $\eta$  is the viscosity of crude oil, mPa·s; B is a constant associated with the properties of crude oil; R is the gas constant, 8.314 J/(mol·K); E is the activation energy, J/mol; T is the temperature, K.

## 3. Results and discussion

## 3.1. Derivation of the structure of asphaltene in crude oil

It is crucial to investigate the catalytic viscosity reduction mechanism of the catalyst on heavy oil at the molecular level and acquire a profound understanding of the main asphaltene molecular structures in heavy oil. Therefore, in this study, FT-ICR MS and ESI were employed to analyze the crude oil. As shown in Fig. 2, the relative molecular mass distribution ranges in the negative (–ESI)

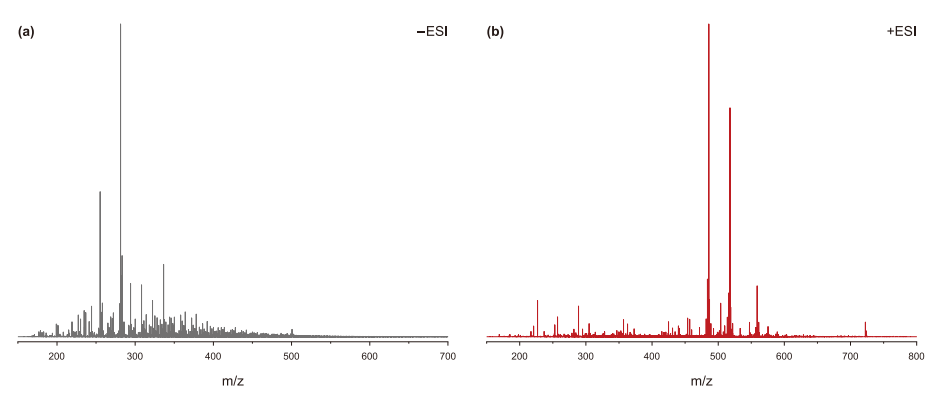


Fig. 2. FT-ICR MS of Crude Oil in -ESI (a) and +ESI (b) conditions.

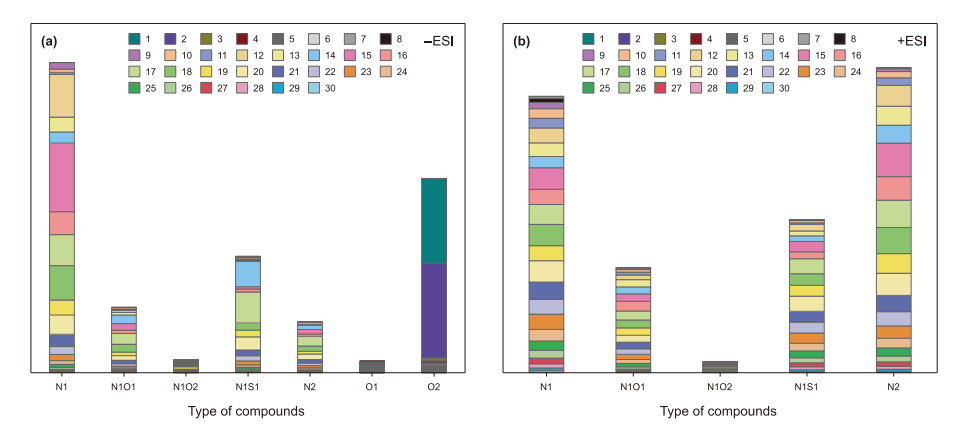


Fig. 3. Relative abundance of various types of compounds in crude oil under -ESI (a) and +ESI (b) conditions.

and positive (+ESI) modes are 150–500 Da and 200–720 Da respectively. Among them, in the –ESI mode, it is mainly concentrated around 300 Da, while in the +ESI mode, it is mainly concentrated around 500 Da, indicating that the overall carbon number of basic nitrogen compounds in the Tahe heavy oil utilized

in this study is higher than that of acidic substances, and the relative molecular mass is larger.

The relative abundances of acidic compounds and basic nitrogen compounds in crude oil are shown in Fig. 3. Compounds are classified into different types (such as N1, N1O1, N1O2, N1S1, N2, O1,

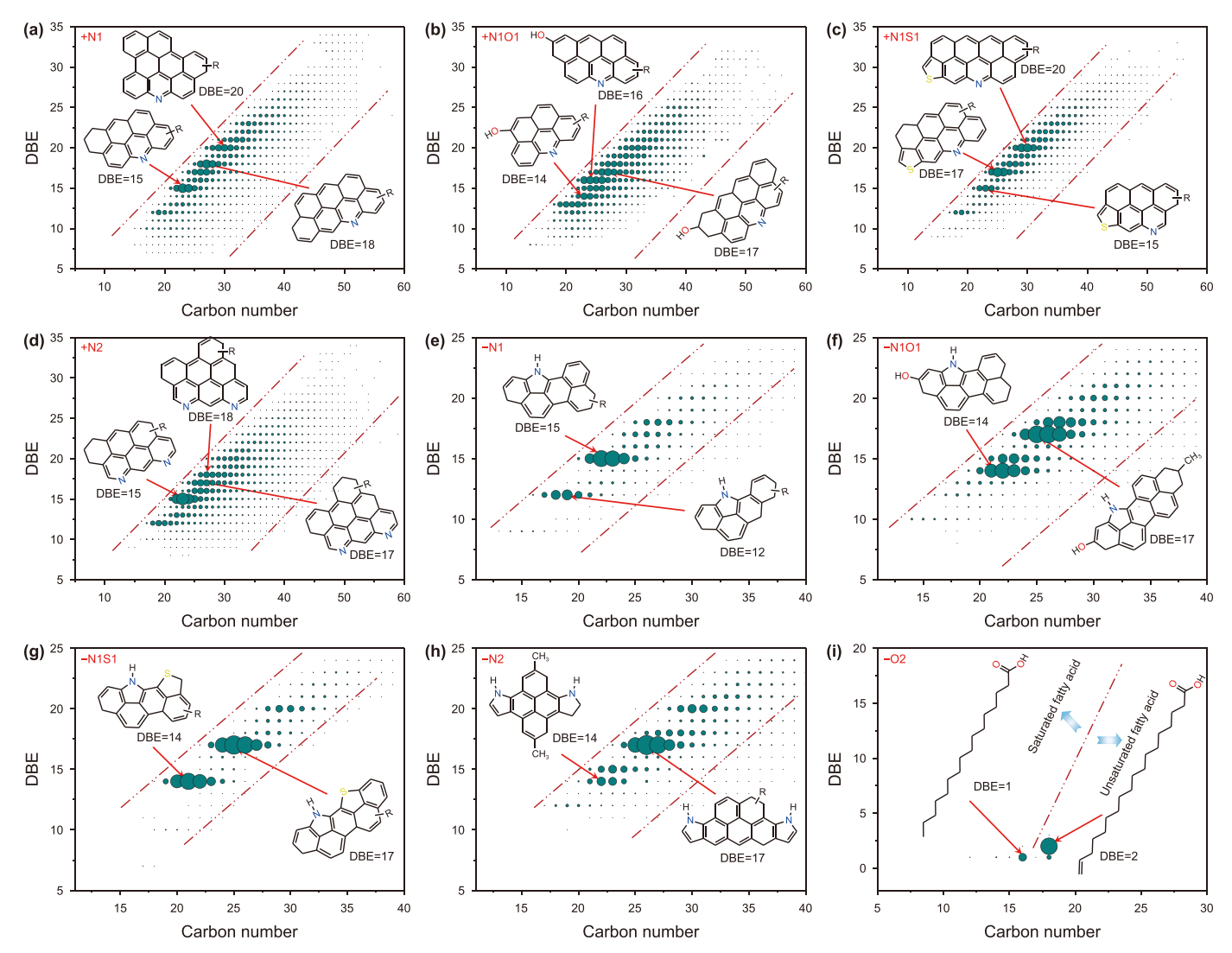


Fig. 4. DBE value-carbon number distribution of different heteroatomic compounds under + ESI (a)-(d) and -ESI (e)-(i) conditions.

and O2) according to the types and numbers of heteroatoms. Different color blocks represent different DBE. Among these, in the –ESI mode, N1 and N2 compounds are mainly neutral nitrogencontaining substances. For example, indole and carbazole substances appear in the negative ion FT-ICR mass spectrum together with acidic components through deprotonation. N1O1 and N1O2 compounds are their corresponding oxides. N1S1 compounds are mainly thiazole or thiophene-pyrrole compounds. O1 compounds are mainly phenolic substances, and O2 compounds are mainly fatty acids or naphthenic acids. In the +ESI mode, N-containing compounds are mainly substances with pyridine rings, such as quinoline, acridine, and their oxides. N1S1 compounds are mainly thiophene-pyridine compounds.

To further elucidate the structures of asphaltenes containing various heteroatoms, this study conducted a DBE value—carbon number distribution analysis on several types of compounds with relatively high abundances in both + ESI and -ESI electrospray ionization modes. The results are shown in Fig. 4, where the size of the points represents the relative abundance of the compounds for a given carbon number and DBE. The larger the point, the higher

the relative abundance. By selecting points with relatively high relative abundances for structural deduction, it was found that the molecular structures in both + ESI and -ESI modes conform to the "island-type" asphaltene structure reported in previous studies (Schuler et al., 2015, 2020). This complex and compact asphaltene structure is a primary factor contributing to the high viscosity of heavy oil. On one hand, the large conjugated system in the molecule enhances  $\pi$ - $\pi$  interactions, promoting molecular aggregation. On the other hand, although the island structure is relatively regular, its compact form creates significant steric hindrance between molecular side chains and functional groups, limiting molecular mobility. Macroscopically, this results in decreased crude oil fluidity and increased viscosity.

# 3.2. Characterization of MOF catalysts

In this study, the morphology and structure of the synthesized MOF catalysts were observed and characterized. Both the SEM and TEM images revealed the thin and flat 2D structure of the MOF catalysts. As shown in Fig. 5, SEM images (Fig. 5(a1), (a2), (b1), and

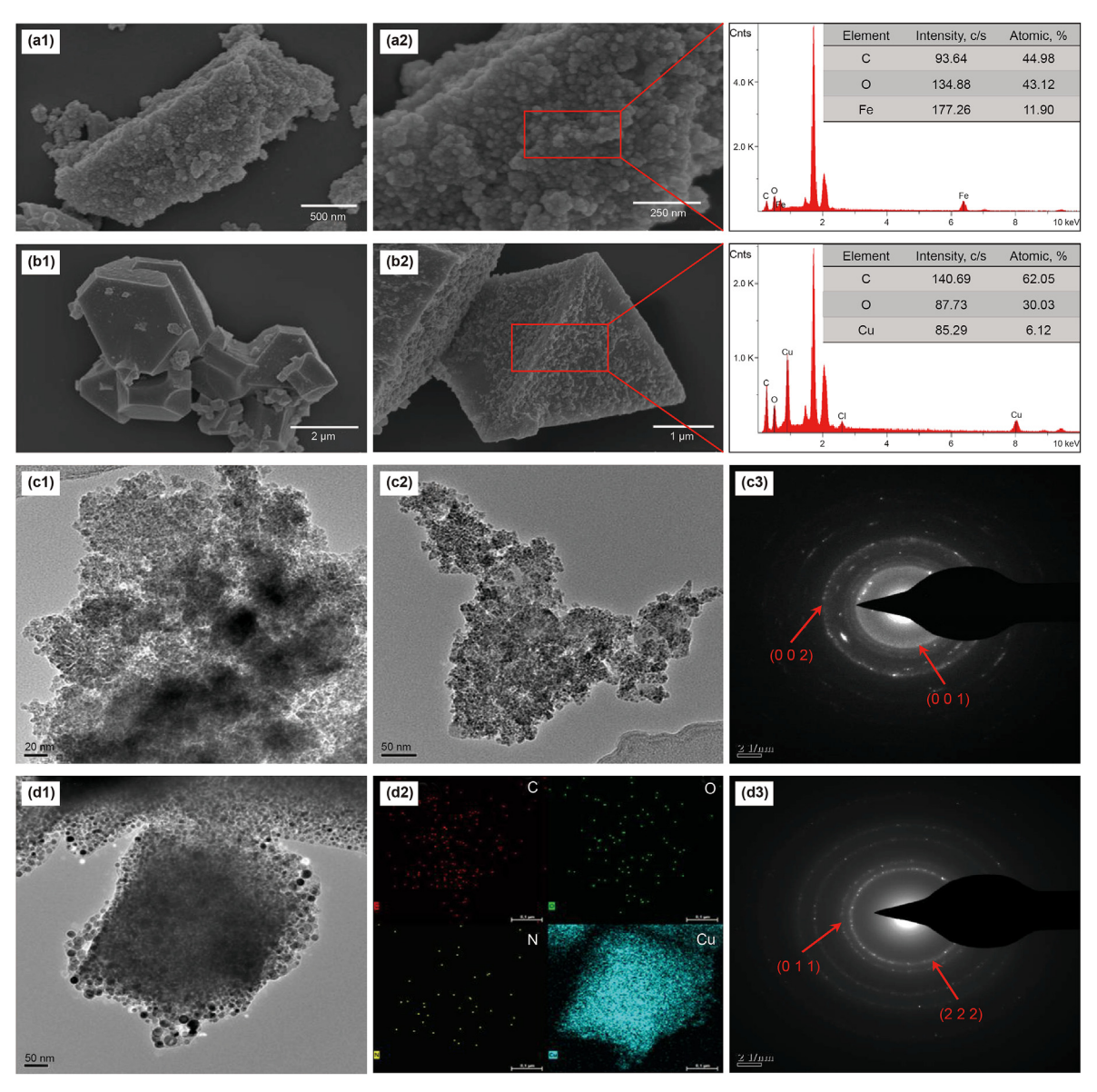


Fig. 5. SEM, TEM, EDS elemental mapping and SAED patterns of Fe-MOF ((a), (c)) and Cu-MOF ((b), (d)) catalysts.

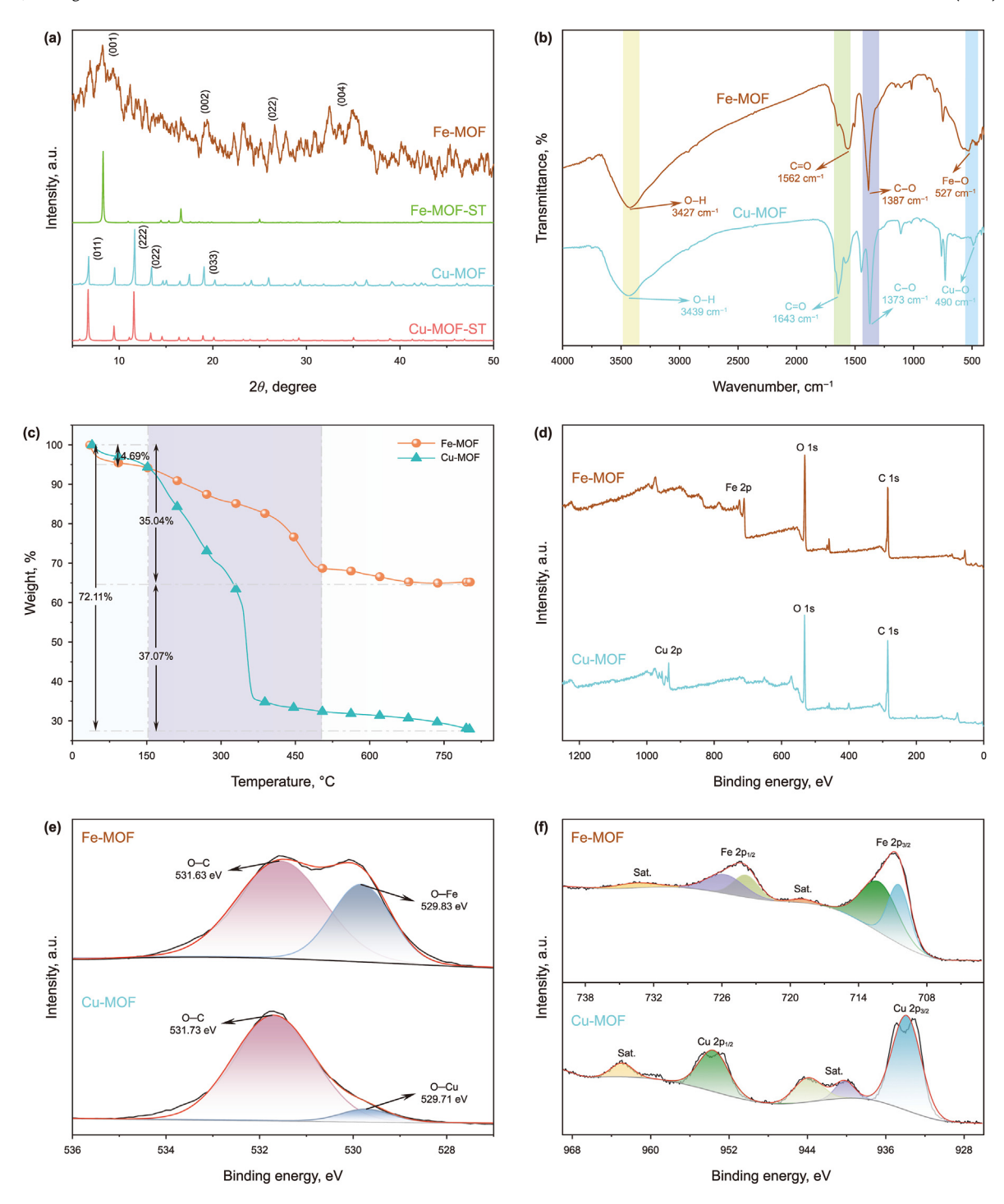


Fig. 6. XRD spectra (a), FT-IR (b), TG curves (c), XPS diagram (d)—(f) of MOF catalysts.

(b2)) demonstrate that the particle size of the synthesized Fe-MOF is approximately 30 nm, and that of Cu-MOF is approximately 600 nm. Both exhibit an obvious layered porous structure. Among them, Fe-MOF appears as microspheres, while Cu-MOF has a regular octahedral structure. Elemental contents of C, O, and Fe/Cu were obtained from the EDS spectra (Fig. 5(a3) and (b3)). To further investigate the internal structure of the catalysts, TEM analysis was performed. As shown in Fig. 5(c1), (c2), and (d1), intact and uniformly distributed nanoparticles of Cu-MOF and Fe-MOF were observed. Fig. 5(d2) displays the EDS spectrum of the Cu-MOF

catalyst, with elemental mapping showing uniform distributions of C, O, N, and Cu (Xu et al., 2024). The diffraction rings in the selected-area electron diffraction (SAED) pattern indicate good crystallinity of the catalyst. Fig. 5(c3) and (d3) reveal the presence of the (011), (222), (001), and (002) planes, which are consistent with the XRD results (Nguyen Sorenson et al., 2020; Zhao et al., 2017). Furthermore, the diffraction rings confirm that the synthesized catalyst is polycrystalline. Compared to single-crystal catalysts, polycrystalline catalysts possess a larger specific surface area and greater corrosion resistance, demonstrating higher efficiency

and longer service life when used for in-situ catalysis of heavy oil (Yang et al., 2023).

The XRD results are presented in Fig. 6(a). For Cu-MOF, characteristic peaks at 6.7°, 11.6°, 13.4°, and 20.1° correspond to the (011), (222), (022), and (033) crystal planes, respectively. Similarly, Fe-MOF exhibits peaks at 8.3°, 16.6°, 25°, and 33.6°, attributed to the (001), (002), (022), and (004) crystal planes. These findings are consistent with previously reported results and align closely with standard reference patterns (Liu et al., 2022; Venu et al., 2020; Zhang et al., 2022). The FT-IR characterization of the MOF catalysts, shown in Fig. 6(b), indicates that the spectra of Fe-MOF and Cu-MOF are generally similar, suggesting that both materials have comparable functional group structures. The peaks at 527 and 490 cm<sup>-1</sup> are attributed to the stretching vibrations of the Fe–O and Cu-O bonds, respectively. This confirms the successful coordination of Fe and Cu elements with oxygen during the synthesis process, which causes the corresponding C-O infrared absorption peak to shift towards the lower frequency region. The peaks at 1387, 1373, 1562, and 1643  $cm^{-1}$  are attributed to the symmetric and asymmetric vibrations of the carboxyl group (-COO-) on the benzene ring of the ligand (Zhang et al., 2024), respectively. The TG of the MOF is shown in Fig. 6(c). The samples were analyzed at a heating rate of 5 °C/min. In the first stage, when the temperature was raised to 150 °C, the catalyst exhibited a weight loss of 4.69%, mainly due to the evaporation of crystallization water and volatile impurities. In the second stage, as the temperature increased

further, the MOF framework began to collapse and degrade. Complete decomposition of Cu-MOF and Fe-MOF occurred at 380 and 500 °C, respectively, with final weight loss rates of 72.11% and 35.04%, respectively. These results suggest that the synthesized MOF catalysts possess good thermal stability and a stable framework structure. Furthermore, Fe-MOF demonstrates superior thermal stability compared to Cu-MOF, XPS analysis was performed to investigate the chemical composition and elemental valence states of the catalyst. The XPS full spectrum in Fig. 6(d) confirms the presence of C, O, Fe, or Cu elements, with no other impurities detected. The O 1s spectrum shown in Fig. 6(e) displays the O-C peak, the O-Fe coordination peak, and the O-Cu coordination peak. The presence of these coordination peaks indicates successful bonding of Fe/Cu elements with the ligand, further confirming the successful preparation of the catalyst. Fig. 6(f) shows the Fe 2p and Cu 2p spectra. The peaks at 711.61 eV and 724.20 eV correspond to Fe  $2p_{3/2}$  and Fe  $2p_{1/2}$ , respectively, with their corresponding satellite peaks at 718.72 eV and 733.12 eV, confirming the existence of  $Fe^{3+}$ . The peaks at 933.66 and 953.57 eV correspond to Cu  $2p_{3/2}$  and Cu  $2p_{1/2}$ , respectively, indicating the divalent structure of Cu-MOF.

#### 3.3. Evaluation of catalyst performance

Under specific conditions, catalytic pyrolysis experiments on heavy oil were conducted using a high-temperature, high-pressure reactor. The catalytic effects and performance of the catalyst were

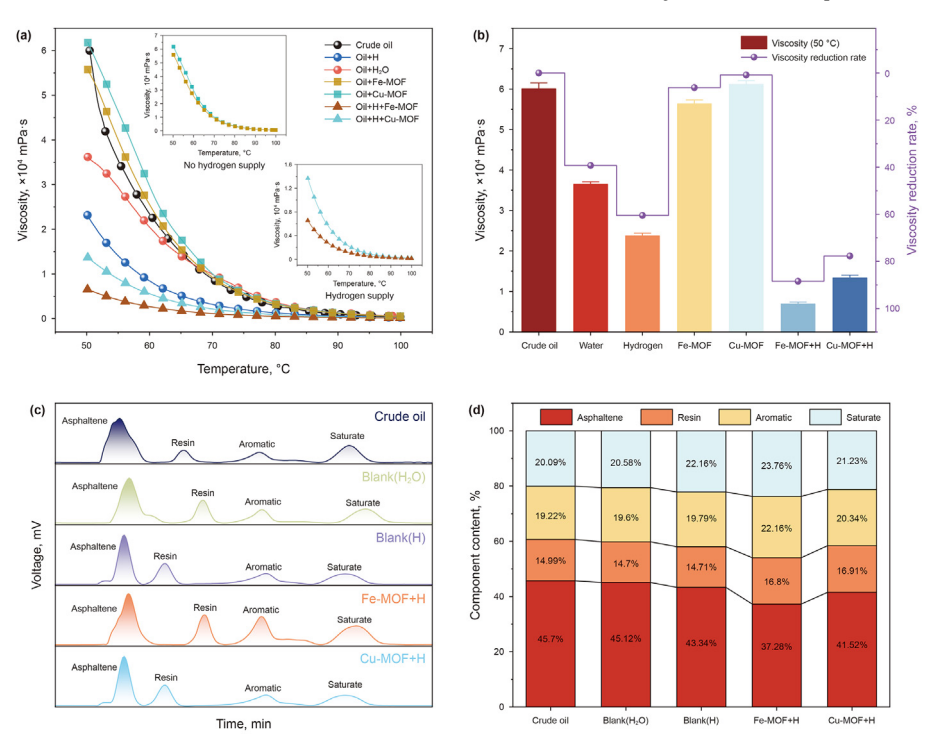
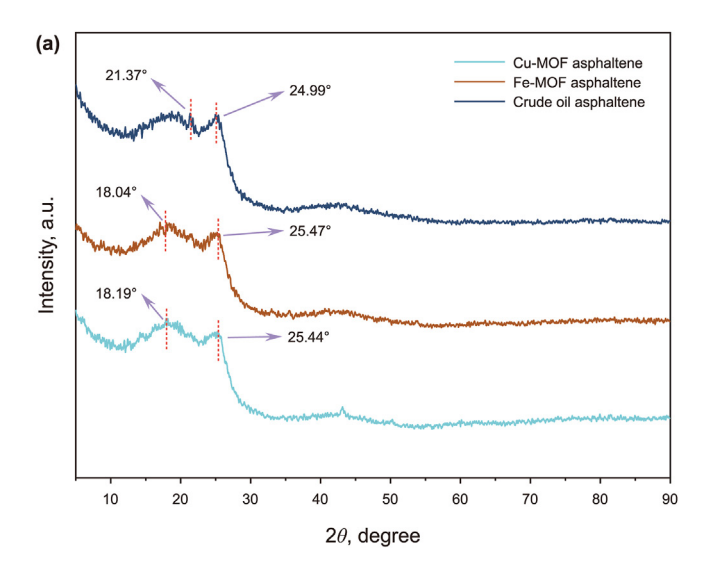
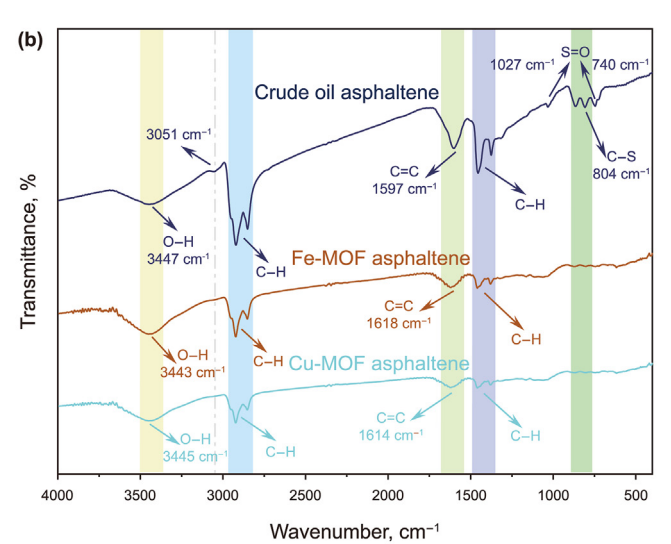


Fig. 7. (a) Viscosity-temperature curve; (b) Viscosity and viscosity reduction at 50 °C; (c)-(d) SARA content of super heavy oil under different conditions.

**Table 2**Comparison of Catalyst for this work with other heavy oil pyrolysis catalysts in recent years.

Catalyst	Extra hydrogen donor	Temperature, °C	Time, h	Viscosity reduction rate, %	Reference
MoO <sub>3</sub> -ZrO <sub>2</sub> /HZSM-5	tetralin	280	24	82.56	Liu et al. (2023)
ZrO <sub>2</sub> -MoO <sub>3</sub>	tetralin	200	24	86.1	Y.Y. Wang et al. (2024)
Ni/N-C-6.0	tetralin	240	24	82.21	Xiong et al. (2022)
NaOH and CuSO <sub>4</sub>	/	300	8	81.43	Zhou et al. (2023)
Cu/BC	1	260	1/3	78.55	Tang et al. (2022)
Fe-MOF	tetralin	160	24	89.09	this work





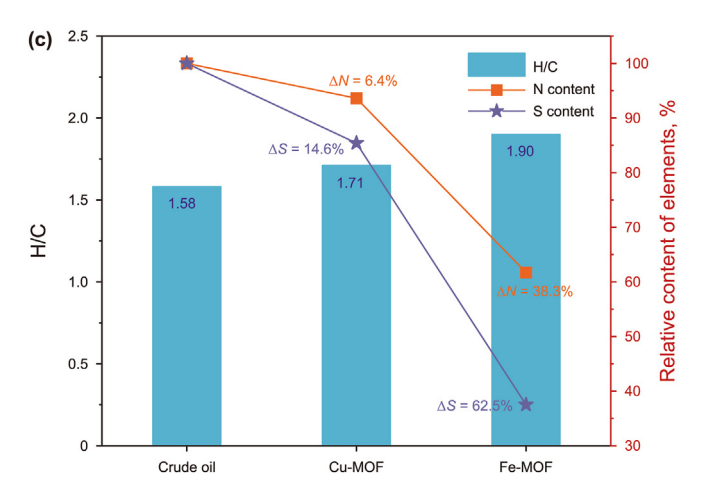


**Fig. 8.** XRD and FT-IR spectra of asphaltenes and elemental analysis of super heavy oil before and after catalyst action.

subsequently evaluated through viscosity-temperature tests, SARA analysis, elemental analysis, and GC-MS.

In this study, water and a hydrogen donor were used as blank controls. Catalytic experiments were conducted both with and without a hydrogen donor, and the corresponding viscosity-

**Table 3** Element content and H/C value of super heavy oil before and after catalysis.

	C, %	Н, %	O, %	N, %	S, %	H/C
Crude oil	84.14	11.06	4.16	0.47	0.48	1.58
Cu-MOF	83.15	11.87	4.13	0.44	0.41	1.71
Fe-MOF	82.56	13.06	3.68	0.29	0.18	1.90

temperature data were measured. The results are shown in Fig. 7(a). In the absence of a hydrogen donor, the viscosity of the heavy oil increased slightly, regardless of whether Fe-MOF or Cu-MOF was used. This increase in viscosity can be attributed to the nanoscale MOF catalysts, which possess a relatively large specific surface area and strong adsorption capacity, causing some macromolecules in the heavy oil or intermediate catalytic products to accumulate on the catalyst surface. The effects of adding only water or only a hydrogen donor on viscosity reduction were minimal. However, the combined effect of the catalyst and hydrogen donor resulted in a significant reduction in the viscosity of the heavy oil. This is because the addition of tetralin promotes the cracking reaction, while the hydrogen radicals it generates facilitate reactions such as hydrogenation saturation, hydrodesulfurization, and hydrodenitrogenation in the presence of the catalyst. In addition, the abundant hydrogen radicals provided by tetralin can quench the free radicals generated during heavy oil pyrolysis, preventing their recombination (Shi et al., 2023). Fig. 7(b) shows the viscosities and viscosity reduction rates of each group at 50 °C. With the addition of a hydrogen donor, the viscosity reduction rates of Fe-MOF and Cu-MOF were 89.09% and 77.21%, respectively. Catalytic pyrolysis also led to changes in the four components of heavy oil. Fig. 7(c) presents the SARA analysis results of heavy oil after catalytic pyrolysis under different conditions. Compared with the blank group, with the addition of catalyst and hydrogen donor, asphaltene molecules in the crude oil became smaller and more dispersed, reducing molecular entanglement and aggregation and thereby significantly decreasing the asphaltene content. The final results are shown in Fig. 7(d). After catalytic pyrolysis, Fe-MOF reduced the asphaltene content by 8.42%, whereas Cu-MOF achieved a reduction of only 4.18%. This difference may be attributed to variations in active sites and thermal stability, which allow Fe-MOF to interact more effectively with asphaltene molecules.

Table 2 lists various catalysts used for heavy oil pyrolysis in recent years. The 2D Fe-MOF synthesized in this study demonstrates excellent viscosity reduction performance under low-temperature conditions, enabling in-situ catalysis in oil reservoirs without additional energy input. This finding highlights the significant application potential of Fe-MOF and suggests its catalytic performance is superior to other catalysts for pyrolysis viscosity reduction.

# 3.4. Analysis of catalytic products

The asphaltene structure is complex, with strong intermolecular interactions and a tendency to aggregate, contributing to the high viscosity of crude oil (Nguyen et al., 2021). To analyze the asphaltene structure before and after catalysis, XRD and FT-IR were performed on asphaltenes separated from the crude oil. Fig. 8(a) presents a comparison of the XRD patterns of asphaltene before and after catalysis. The patterns are largely similar, but the peaks at  $2\theta=24.99^\circ$  and  $2\theta=21.37^\circ$  exhibit noticeable shifts, and the peak shapes have also changed. This suggests that the crystal structure of asphaltene is disrupted after catalysis, affecting its aggregated structure and thereby reducing the viscosity of heavy oil. Fig. 8(b) presents the changes in the infrared spectra of asphaltene before

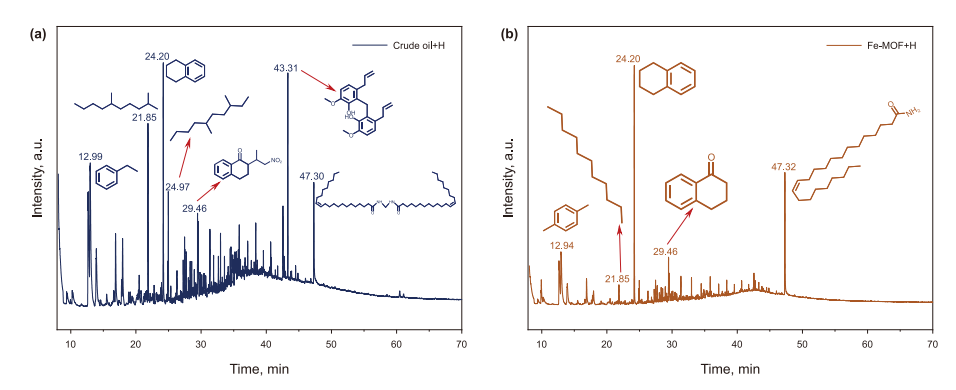


Fig. 9. GC-MS analysis of crude oil and Fe-MOF after catalytic pyrolysis.

**Table 4**Kinetic parameters of each sample fitted by Arrhenius model.

	∆E, KJ/mol	$A, s^{-1}$	Curve fitting	$R^2$
Crude oil	2.89	63.07	2885	0.9829
			$\eta = 63.07 \cdot e RT$	
Cu-MOF	2.80	108.86	2796	0.9631
			$\eta = 108.86 \cdot e^{-RT}$	
Fe-MOF	2.81	91.65	2806	0.9723
			$\eta = 91.65 \cdot e^{-RT}$	
Cu-MOF + H	2.72	19.58	2723	0.9873
			$\eta = 19.58 \cdot e^{-RT}$	
Fe-MOF + H	2.62	12.13	2616	0.9906
			$\eta = 12.13 \cdot e^{-RT}$	

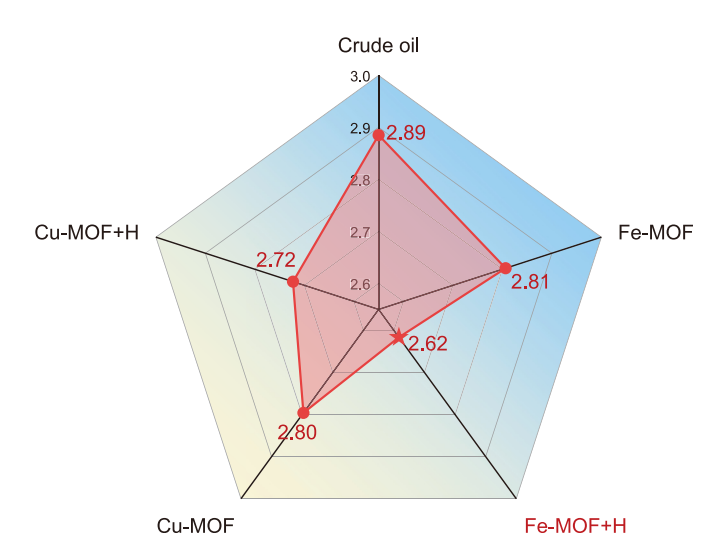


Fig. 10. Activation energy under different catalytic conditions.

and after catalysis. The intensities of the aliphatic stretching vibration peaks of  $-\text{CH}_3$  and  $-\text{CH}_2$  in the range of 3000–2800 cm<sup>-1</sup> are weakened. Indicates that the asphaltenes in the crude oil show side chain breakage after catalyzing, and the broken side chains go into the light components, suggesting that the catalyst promotes the thermal decomposition of asphaltene components. The C=C absorption peak of the aromatic compounds at 1519 cm<sup>-1</sup> is significantly weakened after catalysis, indicating that the catalyst promotes the cracking of the benzene ring. Additionally, the weakening of characteristic peaks in the range of 1300–1500 cm<sup>-1</sup> indicates a reduction in aromatic compound content, suggesting that the catalyst effectively interacts with the benzene ring. The

S=O absorption peaks at 1027 and 740 cm<sup>-1</sup>, along with the C-S absorption peak at 804 cm<sup>-1</sup>, almost completely disappear, demonstrating that the catalyst promotes bond cleavage and facilitates desulfurization, which is consistent with the elemental analysis results. As shown in Fig. 8(c) and Table 3, the contents of N and S elements in heavy oil are significantly reduced after catalysis. This suggests that metal ions in the MOF catalyst interact with N and S atoms, altering their electron cloud densities and making the chemical bonds containing S and N more prone to cleavage, thereby facilitating the removal of N and S elements from heavy oil. Additionally, the results indicate that after catalysis, the H/C ratio increases, the aromatic compound content in crude oil decreases, and macromolecular compounds undergo decomposition and cleavage. With the assistance of the hydrogen donor, the hydrogenation reaction is further enhanced, leading to a reduction in heavy oil viscosity and an improvement in oil product quality.

To elucidate the mechanism of catalytic viscosity reduction, GC-MS was used to analyze the polar substances dissolved in water following the catalytic pyrolysis of heavy oil. As shown in Fig. 9, a substantial amount of organic compounds, including those containing aromatic rings, were dissolved in water after pyrolysis. This indicates that pyrolysis effectively facilitates bond cleavage and enhances dispersion, thereby reducing the viscosity of heavy oil. Secondly, by comparing the pyrolysis results with and without a catalyst, it is evident that the tetralin peak at 24.2 min remains unchanged, while the peak intensities at 21.85, 29.46, and 47.32 min are significantly reduced. Mass spectrometry analysis reveals that, after the addition of the catalyst, macromolecules undergo further cracking, including the detachment of aliphatic hydrocarbon branches and localized groups of aromatic compounds. Moreover, the peaks at 24.97 and 43.31 min almost disappear in the presence of the catalyst, indicating that the catalyst simplifies macromolecular structures, reduces the variety of polar substances, lowers the aromatic compound content in heavy oil, and improves crude oil fluidity (Ma et al., 2023).

## 3.5. Kinetic analysis

#### 3.5.1. Pyrolysis kinetic analysis

The Arrhenius equation was employed to calculate the kinetic parameters of the pyrolysis process, with the fitted results presented in Table 4 and Fig. 10. The findings indicate that the addition of the catalyst lowers the activation energy of heavy oil. Moreover, when both the catalyst and the hydrogen donor are introduced, the activation energy decreases further. This suggests that, under identical conditions, the synergistic effect of the catalyst and the hydrogen donor alters the reaction pathway, significantly reduces the transition state energy, and accelerates the reaction rate.

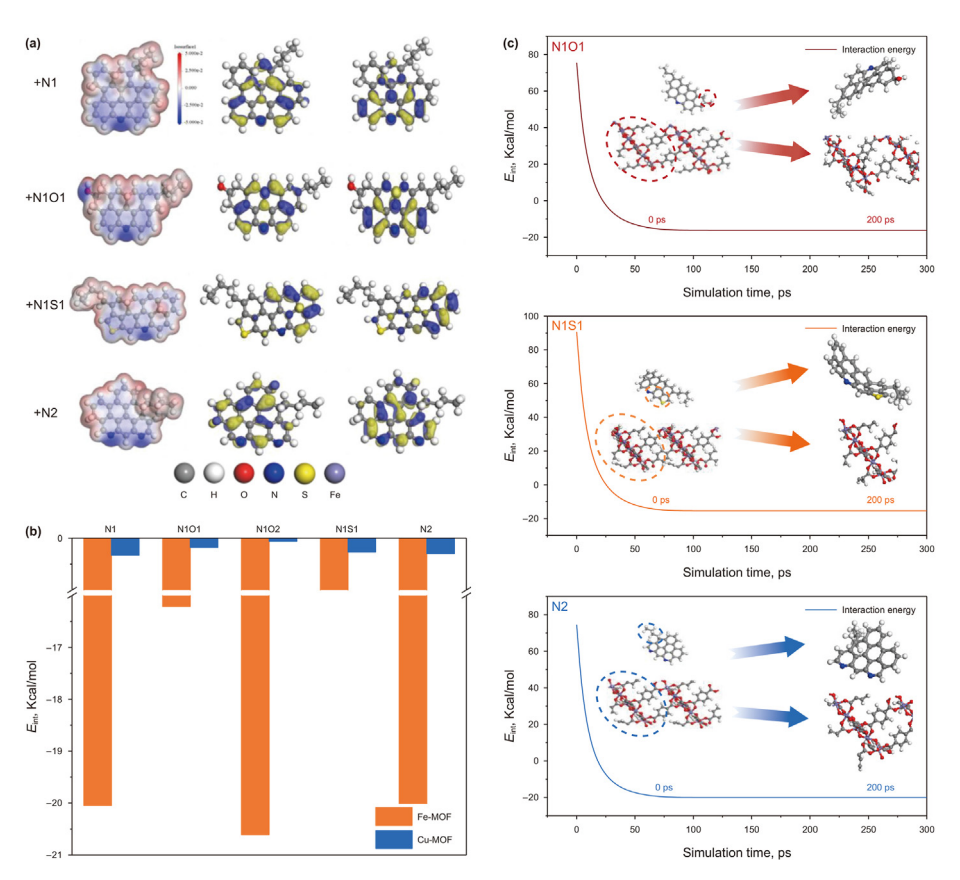


Fig. 11. Molecular dynamics simulation and interaction energy.

# 3.5.2. Molecular dynamics simulation analysis

To further investigate the interaction mechanism between the MOF catalyst and heavy oil, simulations and analyses were conducted using Material Studio software. First, the Dmol3 module was employed to calculate the charges and orbitals of the previously deduced asphaltene molecules. As shown in Fig. 11(a), the energy values of the Highest Occupied Molecular Orbital (HOMO) and Lowest Unoccupied Molecular Orbital (LUMO) are provided in Table 5. The charge calculation results indicate that the electron cloud densities at the heteroatoms in various compounds are generally low, suggesting a tendency to lose electrons. For instance, the p orbital of the sp<sup>2</sup>-hybridized nitrogen atom in the pyridine ring interacts with the p orbitals of the carbon atoms in the ring. forming a conjugated system. This interaction modifies the electron distribution within the molecule, resulting in a relatively lower electron cloud density in the heteroatom region. This finding supports the "island-like" asphaltene molecular structure, which is characterized by a strong conjugation effect. Furthermore, the HOMO and LUMO calculation results reinforce the stability of this structure and corroborate the molecular structure previously hypothesized and deduced through FT-ICR MS analysis (Schuler et al., 2015). Molecular dynamics simulations were performed for 300 ps at 160 °C under NVT (constant volume and temperature) conditions to examine the interactions between various asphaltene molecules

**Table 5**Energy of different types of asphaltene molecules HOMO and LUMO.

	N1	N101	N1S1	N2
E <sub>HOMO</sub> , eV	-0.1559	-0.1586	-0.1611	-0.1532
$E_{\text{LUMO}}$ , eV	-0.0861	-0.0865	-0.0985	-0.0984

and the surface of the MOF catalyst (Kim et al., 2017; Park and Lee, 2022). Conformations were recorded every 1000 steps. Fig. 11(b) illustrates the interaction energies between Fe-MOF and Cu-MOF with different asphaltene molecules. The results reveal that all interaction energies are negative, indicating relatively strong interactions between the MOF catalyst and asphaltene molecules. Among these, the interaction energy between Fe-MOF and the N1O2 type compound is the strongest, reaching -20.61 kcal/mol. Notably, Fe-MOF demonstrates significantly stronger interactions compared to Cu-MOF, aligning with previous findings from viscosity measurements, SARA analysis, elemental analysis, and other assessments. Based on this, the interaction process between Fe-MOF and different asphaltene molecules was further calculated. with the results presented in Fig. 11(c). The calculations reveal that during the interaction process, the surface morphology of the catalyst undergoes significant changes, transitioning from a regular plane to an irregular conformation, accompanied by a notable alteration in the O-Fe-O bond angle. Simultaneously, the spatial structures of the asphaltene molecules also change, including the deformation of six-membered rings and overall molecular distortion. These structural transformations suggest the presence of relatively strong interactions between the catalyst surface and the asphaltene molecules.

## 4. Mechanism analysis

In this study, the possible catalytic mechanism of 2D Fe-MOF for heavy oil was elucidated with the support of experimental characterization and molecular dynamics simulation results, as illustrated in Fig. 12. Fe-MOF features a larger specific surface area on the 2D plane, exposing more active sites and exhibiting higher



Fig. 12. Schematic diagram of catalytic viscosity reduction mechanism of super heavy oil.

electron mobility. This enhances the probability of its d orbitals interacting with the  $\pi$ -electron system of large molecules of heavy oil, thereby lowering the activation energy required for molecular cracking. As a result, this interaction promotes branch breakage, the transformation of long chains into short chains, and the gradual decomposition of macromolecules in heavy oil asphaltene into smaller molecules. Meanwhile, metal ions form coordination bonds with heteroatoms such as N and S in heavy oil, facilitating the adsorption of heavy oil molecules onto the catalyst surface in a specific configuration. Additionally, the porous structure of the MOF enhances adsorption, effectively improving reaction activity and promoting the cleavage of bonds such as C-S and C-N. Consequently, the complex molecules in heavy oil are converted into simpler molecules, and the "island-like" structure transitions from "large islands" and "archipelagos" to "small islands" and "isolated islands", thereby weakening interactions among asphaltene molecules and improving the fluidity of crude oil (Nie et al., 2023; Zhang et al., 2020). Furthermore, the previous test results indicate that the catalytic effect is significantly enhanced when a hydrogen donor is used compared to when it is not. This is because the hydrogen donor generates a substantial amount of hydrogen radicals (H·) during the reaction, which cooperate with the MOF catalyst to facilitate the hydrogenation reaction. On one hand, this increases the content of saturated hydrocarbons and promotes reactions such as desulfurization, denitrification, and demetalization. On the other hand, the hydrogen radicals provided by tetralin quench the free radicals generated during the pyrolysis of heavy oil, preventing their recombination. In summary, the Fe-MOF catalyst demonstrates excellent performance in reducing the viscosity of heavy oil, effectively facilitating its catalytic transformation.

## 5. Conclusion

In this study, 2D Fe-MOF and Cu-MOF were synthesized using a simple, environmentally friendly stirring method at room temperature, followed by comprehensive characterization analyses. The catalytic effects of these catalysts on viscosity reduction in Tahe heavy oil were systematically evaluated. Under conditions of

160 °C, a catalyst concentration of 0.5 wt%, and a hydrogen donor (tetralin) concentration of 2 wt%, both catalysts effectively facilitated in-situ catalytic pyrolysis, significantly reducing the viscosity of heavy oil. Among them, Fe-MOF achieved a remarkable viscosity reduction rate of 89.09% while simultaneously decreasing the asphaltene content by 8.42%. The structural deduction of heavy oil asphaltene indicates that different asphaltene molecules conform to an "island-like" structure. This feature accounts for the high viscosity of heavy oil at the molecular level and serves as a foundational model for molecular dynamics simulations. The research findings reveal that the d orbitals of metal ions in Fe-MOF interact with the  $\pi$ -electron system of heavy oil macromolecules, reducing the activation energy for molecular cracking and facilitating the progressive decomposition of macromolecules in heavy oil asphaltene into smaller molecules. Furthermore, the coordination effect and pore structure of Fe-MOF enhance the cleavage of chemical bonds such as C-S and C-N, efficiently transforming complex heavy oil molecules into simpler ones. Most importantly, the synergistic effect between the Fe-MOF catalyst and the hydrogen donor significantly enhances the hydrogenation reaction, further reducing the viscosity of heavy oil. In summary, the catalyst synthesized in this study demonstrates high efficiency in in-situ catalysis of heavy oil, providing a valuable basis for the exploitation and utilization of heavy oil resources and exhibiting broad application potential.

# **CRediT authorship contribution statement**

**Chi Li:** Writing — original draft, Methodology, Investigation, Formal analysis, Conceptualization. **Ji-Xiang Guo:** Writing — review & editing, Methodology, Investigation, Conceptualization. **Li Wang:** Visualization, Investigation. **Wen-Long Zhang:** Supervision, Resources. **Peng-Cheng Xue:** Writing — review & editing. **Chen-Hao Gao:** Validation, Software.

## **Conflict of interest**

All authors disclosed no relevant relationships.

#### **Acknowledgments**

This study was financially supported by the National Natural Science Foundation of China (52174047) and Sinopec Project (No. P23138).

#### References

- Elahi, S.M., Scott, C.E., Chen, Z.X., Pereira-Almao, P., 2019. In-situ upgrading and enhanced recovery of heavy oil from carbonate reservoirs using nano-catalysts: upgrading reactions analysis. Fuel 252, 262–271. https://doi.org/10.1016/ i.fuel.2019.04.094.
- Ge, K., Sun, S.J., Zhao, Y., Yang, K., Wang, S., Zhang, Z.H., Cao, J.Y., Yang, Y.F., Zhang, Y., Pan, M.W., Zhu, L., 2021. Facile synthesis of two-dimensional iron/cobalt metal—organic framework for efficient oxygen evolution electrocatalysis. Angew. Chem. Int. Ed. 60 (21), 12097–12102. https://doi.org/10.1002/anie.202102632.
- Goshayeshi, B., Theofanidis, S.A., Abbas-Abadi, M.S., Mahmoudi, E., Akin, O., Varghese, R.J., Lemonidou, A., Van Geem, K.M., 2024. Selective catalytic conversion of model olefin and diolefin compounds of waste plastic pyrolysis oil: insights for light olefin production and coke minimization. Chem. Eng. J. 500, 156987. https://doi.org/10.1016/j.cej.2024.156987.
- Guo, W., Fan, C.H., Liu, Z., Zhang, X., Sun, Y.H., Li, Q., 2024. Fates of pyrolysis oil components in the non-isothermal propped fractures during oil shale in situ pyrolysis exploitation. Energy 288, 129851. https://doi.org/10.1016/j.energy.2023.129851.
- Kim, S.H., Kim, K.D., Lee, H., Lee, Y.K., 2017. Beneficial roles of H-donors as diluent and H-shuttle for asphaltenes in catalytic upgrading of vacuum residue. Chem. Eng. J. 314, 1–10. https://doi.org/10.1016/j.cej.2016.12.119.
- Karnjanakom, S., Suriya-umporn, T., Bayu, A., Kongparakul, S., Samart, C., Fushimi, C., Abudula, A., Guan, G.Q., 2017. High selectivity and stability of mg-doped Al-MCM-41 for in-situ catalytic upgrading fast pyrolysis bio-oil. Energy Convers. Manag. 142, 272–285. https://doi.org/10.1016/j.enconman.2017.03.049.
- Khorasani, M., Sarker, S., Kabir, G., Ali, S.M., 2022. Evaluating strategies to decarbonize oil and gas supply chain: implications for energy policies in emerging economies. Energy 258, 124805. https://doi.org/10.1016/j.energy.2022.124805.
- Lin, D., Zhu, H.H., Wu, Y.N., Lu, T., Liu, Y.B., Chen, X.B., Peng, C., Yang, C.H., Feng, X., 2019. Morphological insights into the catalytic aquathermolysis of crude oil with an easily prepared high-efficiency Fe<sub>3</sub>O<sub>4</sub>-containing catalyst. Fuel 245, 420–428. https://doi.org/10.1016/j.fuel.2019.02.063.
- Li, F.H., Sweeney, D.J., Dai, Y.J., Wang, C.H., 2021. Effect of novel Ni<sub>2</sub>P-loaded catalysts on algal pyrolysis bio-oil. Renew. Sustain. Energy Rev. 151, 111575. https:// doi.org/10.1016/j.rser.2021.111575.
- Lin, Y.T., Li, Y.H., Cao, Y., Wang, X.Z., 2021. Two-dimensional mofs: design & synthesis and applications. Chem. Asian J. 16 (21), 3281–3298. https://doi.org/10.1002/asia.202100884.
- Liu, J., Yuan, Y., Cheng, Y.N., Fu, D.A., Chen, Z.Y., Wang, Y., Zhang, L.F., Yao, C.D., Shi, L., Li, M.Y., Zhou, C., Zou, M.Z., Wang, G.B., Wang, L., Wang, Z., 2022. Copper-based metal—organic framework overcomes cancer chemoresistance through systemically disrupting dynamically balanced cellular redox homeostasis. J. Am. Chem. Soc. 144 (11), 4799—4809. https://doi.org/10.1021/jacs.1c11856.
- Liu, R.Q., Zhang, L.Q., Pan, H.D., Wang, Y.Y., Li, J.Y., Wang, X.W., Yang, Z.D., Han, X.L., Lin, R.Y., 2023. Study on the in situ desulfurization and viscosity reduction of heavy oil over MoO<sub>3</sub>–ZrO<sub>2</sub>/HZSM-5 catalyst. Pet. Sci. 20 (6), 3887–3896. https://doi.org/10.1016/j.petsci.2023.08.005.
- Liang, C.J., Liu, R.R., Zhao, R.Y., Hou, X.X., Zhao, Y.X., Yang, J., Wang, T., Chen, T., Ding, W.P., 2023. A review: multi-hierarchy design strategy of electrocatalysts for energy molecule conversion. J. Energy Chem. 86, 54–68. https://doi.org/ 10.1016/j.jechem.2023.06.034.
- Li, J.J., Yang, Z., Deng, G.Z., Yang, F.X., Wang, S.G., Tang, X.D., 2024. In-situ hydrothermal upgrading and mechanism of heavy oil with nano-Fe<sub>2</sub>O<sub>3</sub> in the porous media. J. Anal. Appl. Pyrolysis 183, 106757. https://doi.org/10.1016/j.jaap.2024.106757.
- Ma, L.W., Slaný, M., Guo, R., Du, W.C., Li, Y.F., Chen, G., 2023. Study on synergistic catalysis of ex-situ catalyst and in-situ clay in aquathermolysis of water-heavy oil-ethanol at low temperature. Chem. Eng. J. 453, 139872. https://doi.org/ 10.1016/j.cej.2022.139872.
- Mukhamatdinov, I.I., Mahmoud, A.R., Affane, B., Mukhamatdinova, R.E., Sitnov, S.A., Vakhin, A.V., 2023. Development of a nanodispersed catalyst based on iron and nickel for in situ upgrading Ashal'cha heavy oil. Energy & Fuels 37 (18), 13912–13927. https://doi.org/10.1021/acs.energyfuels.3c02257.
- Nguyen Sorenson, A.H.T., Wu, Y., Orcutt, E.K., Kent, R.V., Anderson, H.C., Matzger, A.J., Stowers, K.J., 2020. Energetic decomposition yields efficient bimetallic Cu MOF-derived catalysts. J. Mater. Chem. A. 8 (30), 15066–15073. https://doi.org/10.1039/DOTA04765A.
- Nguyen, M.T., Nguyen, D.L.T., Xia, C.L., Nguyen, T.B., Shokouhimehr, M., Sana, S.S., Grace, A.N., Aghbashlo, M., Tabatabaei, M., Kim, S.Y., Lam, S.S., Le, Q.V., 2021. Recent advances in asphaltene transformation in heavy oil hydroprocessing: Progress, challenges, and future perspectives. Fuel Process. Technol. 213, 106681. https://doi.org/10.1016/j.fuproc.2020.106681.
- Nie, F.H., Jian, W., Yu, Z.C., Chow, C.L., Lau, D., 2023. Mesoscale modeling to study isolated asphaltene agglomerates. Constr. Build. Mater. 379, 131249. https:// doi.org/10.1016/j.conbuildmat.2023.131249.

Park, J.W., Lee, K.B., 2022. Molecular dynamics simulations of asphaltene aggregation in heavy oil system for the application to solvent deasphalting. Fuel 323, 124171. https://doi.org/10.1016/j.fuel.2022.124171.

- Razavian, M., Fatemi, S., 2021. Catalytic evaluation of metal azolate framework-6 in pristine and metal doped modes in upgrading heavy residual fuel oil. J. Anal. Appl. Pyrolysis 156, 105093. https://doi.org/10.1016/j.fuel.2023.130535.
- Schuler, B., Meyer, G., Peña, D., Mullins, O.C., Gross, L., 2015. Unraveling the molecular structures of asphaltenes by atomic force microscopy. J. Am. Chem. Soc. 137 (31), 9870–9876. https://doi.org/10.1021/jacs.5b04056.
- Scheele-Ferreira, E., Scott, C.E., Perez-Zurita, M.J., Pereira-Almao, P., 2017. Effects of the preparation variables on the synthesis of nanocatalyst for in situ upgrading applications. Ind. Eng. Chem. Res. 56 (25), 7131–7140. https://doi.org/10.1021/ acs.iecr.7b01107.
- Schuler, B., Zhang, Y.L., Liu, F., Pomerantz, A.E., Andrews, A.B., Gross, L., Pauchard, V., Banerjee, S., Mullins, O.C., 2020. Overview of asphaltene nanostructures and thermodynamic applications. Energy & Fuels 34 (12), 15082–15105. https://doi.org/10.1021/acs.energyfuels.0c00874.
- Shi, H., Mao, Z.Q., Ran, L.C., Ru, C.D., Guo, S.W., Dong, H., 2023. Heavy oil viscosity reduction through aquathermolysis catalyzed by Ni<sub>20</sub>(NiO)<sub>80</sub> nanocatalyst. Fuel Process. Technol. 250, 107911. https://doi.org/10.1016/j.fuproc.2023.107911.
- Tang, X.D., He, B., Li, J.J., Qin, G.F., 2022. One-step preparation of Cu/BC catalyzed the upgrading of heavy oil assisted by microwave. J. Petrol. Sci. Eng. 208, 109683. https://doi.org/10.1016/j.petrol.2021.109683.
- Venu, B., Shirisha, V., Vishali, B., Naresh, G., Kishore, R., Sreedhar, I., Venugopal, A., 2020. A Cu-BTC metal—organic framework (MOF) as an efficient heterogeneous catalyst for the aerobic oxidative synthesis of imines from primary amines under solvent free conditions. New J. Chem. 44 (15), 5972–5979. https://doi.org/10.1039/C9N(05997K.
- Wang, Q., Astruc, D., 2020. State of the art and prospects in metal—organic framework (MOF)-based and MOF-derived nanocatalysis. Chem. Rev. 120 (2), 1438–1511. https://doi.org/10.1021/acs.chemrev.9b00223.
- Wang, L., Guo, J.X., Zhang, X.J., Gao, C.H., Xiong, R.Y., Kiyingi, W., Luo, D., 2023. Nanoscale mof-catalyzed pyrolysis of oil shale and kinetic analysis. J. Anal. Appl. Pyrolysis 174, 106149. https://doi.org/10.1016/j.jaap.2023.106149.
- Wang, C.H., Gao, L.Y., Liu, M.H., Nian, Y., Shu, Q.L., Xia, S.Q., Han, Y., 2024. Viscosity reduction mechanism of surface-functionalized Fe<sub>3</sub>O<sub>4</sub> nanoparticles in different types of heavy oil. Fuel 360, 130535. https://doi.org/10.1016/j.fuel.2023.130535.
- Wang, L., Guo, J.X., Xiong, R.Y., Gao, C.H., Zhang, X.J., Luo, D., 2024. In situ modification of heavy oil catalyzed by nanosized metal-organic framework at mild temperature and its mechanism. Chin. J. Chem. Eng. 67, 166–173. https://doi.org/10.1016/j.cjche.2023.11.023.
- Wang, Y.Y., Lin, R.Y., Zhang, L.Q., Han, X.L., Li, J.Y., Huang, C.X., Dong, Q.W., Chen, P.Y., Li, H.N., Wang, X.W., 2024. ZrO<sub>2</sub>-MoO<sub>3</sub>/modified lotus stem biochar catalysts for catalytic aquathermolysis of heavy oil at low-temperature. Fuel 357, 129597. https://doi.org/10.1016/j.fuel.2023.129597.
- Xue, Y.P., Zhao, G.C., Yang, R.Y., Chu, F., Chen, J., Wang, L., Huang, X.B., 2021. 2D metal—organic framework-based materials for electrocatalytic, photocatalytic and thermocatalytic applications. Nanoscale 13 (7), 3911–3936. https://doi.org/10.1039/D0NR09064F.
- Xue, L., Liu, P.C., Zhang, Y., 2022. Development and research status of heavy oil enhanced oil recovery. Geofluids 2022 (1), 5015045. https://doi.org/10.1155/ 2022/5015045.
- Xiong, P., Yang, H.Y., Wu, P.Y., Liao, Y.Q., Tan, D.C., Ma, Z.F., Yan, X.M., 2022. Study on catalytic aquathermolysis of heavy oil by simple synthesis of highly dispersed nickel-loaded nitrogen-doped carbon catalysts. Mol. Catal. 529, 112528. https:// doi.org/10.1016/j.mcat.2022.112528.
- Xu, S.Y., Li, M., Li, Z.Y., Ding, M.J., Wang, Y.J., Jin, Z.L., 2024. Coal-based carbon quantum dots modified ni-mof and Co/Zr-MOF heterojunctions for efficient photocatalytic hydrogen evolution. Int. J. Hydrogen Energy 70, 666–676. https://doi.org/10.1016/j.ijhydene.2024.05.235.
- Yang, H.B., Guo, J.Z., Chu, L., Huang, Z., Liu, Z.H., Wang, L.Y., Wang, Z.K., Yang, M., Wang, G., 2023. Self-assembly of Fe-MOF on vermiculite nanosheets with enhanced catalytic activity. Appl. Clay Sci. 245, 107138. https://doi.org/10.1016/iclay.2023.107138
- Zhao, K., Liu, Y.M., Quan, X., Chen, S., Yu, H.T., 2017. CO<sub>2</sub> electroreduction at low overpotential on oxide-derived Cu/carbons fabricated from metal organic framework. ACS Appl. Mater. Interfaces 9 (6), 5302–5311. https://doi.org/ 10.1021/acsami.6b15402.
- Zhang, Y.L., Siskin, M., Gray, M.R., Walters, C.C., Rodgers, R.P., 2020. Mechanisms of asphaltene aggregation: Puzzles and a new hypothesis. Energy & Fuels 34 (8), 9094–9107. https://doi.org/10.1021/acs.energyfuels.0c01564.
- Zhang, J.J., Tang, F.M., Wan, K.C., Yang, Y.G., Zhang, C.M., Ming, P.W., Li, B., 2022. MOF-derived CoFe alloy nanoparticles encapsulated within N,O Co-doped multilayer graphitized shells as an efficient bifunctional catalyst for zinc-air batteries. J. Mater. Chem. A. 10 (28), 14866–14874. https://doi.org/10.1039/ D2TA02957].
- Zhang, M.Y., Wu, Y.J., Han, X., Zeng, Y.M., Xu, C.C., 2022. Upgrading pyrolysis oil by catalytic hydrodeoxygenation reaction in supercritical ethanol with different hydrogen sources. Chem. Eng. J. 446, 136952. https://doi.org/10.1016/ j.cej.2022.136952.
- Zhang, X.J., Guo, J.X., Gao, C.H., Kiyingi, W., Wang, L., Fei, D.T., Peng, Z.Y., Li, J.M., Dong, J.F., 2023. A molecular study of viscosity-causing mechanism and viscosity reduction through re-emulsification for jimsar shale oil. J. Mol. Liq. 392, 123470. https://doi.org/10.1016/j.molliq.2023.123470.

- Zhou, Y.T., Zhao, Q.Y., Miao, Y., Wang, X.T., Zhang, Y.L., Wang, Y.C., Guo, L.J., 2023. Study on the synergistic effect of NaOH and CuSO<sub>4</sub> in aquathermolysis upgrading. Fuel Process. Technol. 244, 107715. https://doi.org/10.1016/j.fuproc.2023.107715.
- J. Luproc. 2023.107/15.

  Zhang, Z.W., Liu, C., Chen, Y.L., Chen, Q., Shi, Y.Z., Wang, Z.W., Bi, J.H., Yu, J.C., Wu, L., 2024. Defect modulation of MIL-68(Fe) MOFs by Cu doping for boosting photocatalytic N<sub>2</sub> fixation. J. Catal. 432, 115436. https://doi.org/10.1016/j.jcat.2024.115436.
- Zhou, Y.T., Zhao, Q.Y., Wang, X.T., Miao, Y., Song, Z.W., Jin, H., Guo, L.J., 2024. Investigation on the effect of hydrothermal reaction with CuSO<sub>4</sub> on rheological property of heavy oil. Constr. Build. Mater. 411, 134294. https://doi.org/10.1016/j.conbuildmat.2023.134294.
- Zhou, Z.C., Li, X.F., Gao, K., Nan, J., Xiao, H., Lu, Y.K., Li, B.F., Chai, Y.M., Wang, J.Q., 2025. A review on the reaction mechanism of heavy oil catalytic aquathermolysis: Carbocationic reactions or free radical reactions? J. Anal. Appl. Pyrolysis 186, 106923. https://doi.org/10.1016/j.jaap.2024.106923.